Decimeter and infrared radiation of lower ionosphere at a period of high solar activity

Golubkov G.V., Manzhelii M.I.
Semenov Institute of Chemical Physics of Russian Academy of Sciences, Moscow, Russia
Golubkov@chph.ras.ru

Introduction

At a period of enhanced solar activity, the error in positioning of global navigational satellite systems increases. This occurs both during short (of 5-20 min duration) and prolonged (several hours) time periods. In the first case, errors arise due to the radiation coming from the solar flare. The second situation happens under the action of solar wind within 30-35 hours after the flare. An example is the time dependence of the Global Positioning System (GPS) operation at a period of enhanced solar activity published on the website of the Cornell University [1]. According to the data of real-time measurements made at the monitoring stations of the Arecibo observatory (Puerto Rico) in the year 2011, a 20-min interruption in the GPS was observed routinely from August 30 to September 2 between 03.00 and 04.00 UTC. In these measurements, the horizontal positioning error reached 50 m and up.

For the stronger geomagnetic disturbances, the GPS signal can fully disappear over a long period [1]. For instance, according to the data obtained in September 15-16 2011 at the Sao Luis Observatory (Brazil), the GPS signal disappeared more than once during a day. At a period from 16.00 UTC September 15 to 01.00 UTC September 16, the signal at receiver disappeared five times sporadically for 5-30 minutes. Over those days, the horizontal positioning error significally exceeded 50 m.

It was shown in [2] that, for solar flares of different intensity, the signal-to-noise ratio decreases, in a certain sequence, for frequencies $L_1 = 1.57542$ and $L_2 = 1.22760$ GHz. For the flare of level X-1 (22.15 UTC December 14, 2006) the signal-to-noise ratio decreased for the L_1 frequency. At the same time, this ratio remained constant for the L_2 frequency. The X-3 flare (02.40 UTC December 13, 2006) resulted in a simultaneous decrease in the signal-to-noise ratio for both frequencies. The duration of the observed phenomena was about 30 minutes in both cases. An increase in the signal intensity at the GPS receiver in a period of enhanced solar activity is another phenomenon worthy of noting. The time dependences of the GPS-signal intensity at the receiver and the integral number of failures at the receiver during the course of the geomagnetic disturbance July 15, 2000, are given in [3]. The signal intensity at the receiver was found to increase approximately by a factor of three relative to the intensity of the transmitter signal. As the signal intensity at receiver increased, the integral number of failures also increased. No explanation was given by the authors of the cited works for the cause of the increase in intensity.

The detection of intense IR radiation in the range from 10 to 40 μm, first measured by the FIRST spectrometer in June 7, 2005 [4], is no less interesting fact, as shown below. In this work, an explanation of the above-mentioned phenomena is suggested on a basis of the physicochemical processes occurring in a nonequilibrium two-temperature plasma in the E and D layers of the Earth.

Traditional models of ionospheric processes based on the total electron content and wave optics during geomagnetic disturbances of the ionosphere are ineffective [5]. The optical quantum resonant properties of the neutral medium of a low ionosphere, where the influence on the satellite signal propagation is most appreciable, are began to investigate recently (see, for example, [6-9]). Simultaneous analysis of the additional background noise and the signal propagation delay time, which determines the positioning error, can be a promising approach to

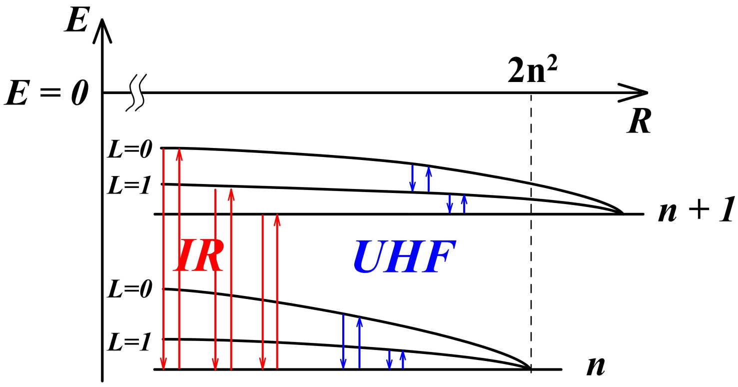

Fig. 1. Potential energy curves of the quasimolecule A**M

the study of such properties. Using of standard methods of measurement noise cannot detect a number of physicochemical reactions in the lower ionosphere responsible for its formation and influencing on positioning errors [6, 8]. To solve this problem, it is convenient to bond the level of background noise to the measured signal of GPS, since the propagation delay is associated with the manifestation of the most important atmospheric process: l - the mixing of highly excited states [7, 9]. For this purpose, it is advisable to define the signal / noise ratio (C/N) thus, when as signal should be understand the level of the selected signal receiver GPS, and as the value of its noise level we must choose the value of its fluctuations. Finding ways to ensure the sustainability of the system GPS, is a fundamental scientific and technical problem. In this paper we present one of the possible options for its solutions by choosing another range of carrier frequencies.

Rydberg states in neutral medium

Solar flares generate additional background ultrahigh-frequency (UHF) radiation in the lover ionosphere which is caused by the radiative transitions between the Rydberg states of particles excited in a neutral medium under the action of solar flux or flow of electrons ejected from the ionosphere [10]. By Rydberg states are called those highly excited atomic and molecular states which are situated near the ionization threshold and characterized by an infinite sequence of energy levels converging to the threshold. They are intermediate between the low-lying excited states and the ionized states in the continuum spectrum. The Rydberg atoms and molecules have one excited weakly bound electron whose state is classified by an energy level with principal quantum number n and electronic angular momentum l about the ion core. The energies of the levels with high angular momenta do not depend on l (orbitally degenerate states). These states are the most stable statistically, because electron resides mostly at a large distance from the ion core.

The process giving rise to the degenerate states with high electronic angular momenta is referred to as l -mixing. It proceeds rapidly and irreversibly in the lower ionosphere. As a result, the quantum distinctions between the excited atoms and molecules disappear and the radiation spectrum becomes independent of their chemical composition [11]. The l -mixing process proceeds in a rather dense neutral gaseous medium with a density exceeding 10^{12} cm^{-3}, which corresponds to altitudes of $h \leq 120$ km. The corresponding efficiency criterion directly related to the density of medium is that, at least, one neutral molecule M occurs in the electron cloud of a Rydberg particle A** (of radius $2n^2a_0$, where a_0 is the Bohr radius). The interaction between them gives rise to quasimolecules A**M whose potential curves are splitted from the degenerate Coulomb levels and classified by the index L characterized the amplitude of elastic electron scattering on the neutral molecule M. Each of them includes a superposition of Rydberg

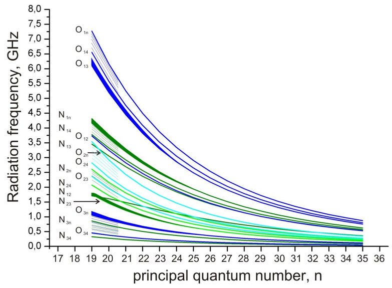

Fig. 2. UHF radiation lines of the A**N_2 and A**O_2 quasimolecules

states with different values of l [11]. The energy scheme of potential curves dependent on the interatomic coordinate R is given in Fig.1 for the quantum L - states with angular momenta $L = 0$ and $L = 1$ that are split out from the degenerate Coulomb n+1 and n levels in the classical turning points. The optical transitions without changing principal quantum number ($\Delta\, n = 0$) between the split-out and degenerate states of quasimolecules A**M are shown by blue arrows. They correspond to the UHF radiation in the decimeter range. The red arrows indicate analogous transitions with a change in the principal quantum number $\Delta\, n = 1$ to produce IR radiation.

At altitudes $h \leq 50$ km, the Rydberg states of particles $A**$are unoccupied because of the quenching due to the interaction of Rydberg particles $A**$ with unexcited oxygen molecules and to the formation of an intermediate ionic complex $A^+(n\,L)\,O_2^-\,(s)$ (harpoon mechanism), i.e.,

$$A^{**}(n\,L)\;+\;O_2\;\rightarrow\;A^+(n\,L)\,O_2^-\,(s)\rightarrow\;A^{**}(n'\,L')\;+\;O_2,$$

(s is the vibrational quantum number). The reason is that the negative molecular ion O_2^- has a number of resonant vibrationally excited autoionizing levels situated against the background of ionization continuum. Based on these two circumstances, one can suggest that the atmospheric layer radiating in the decimeter range forms between 50 and 120 km.

Nonequilibrium two-temperature recombining plasma

An increase in the solar activity gives rise to two types of nonequilibrium plasma in the ionospheric E and D layers: *recombining* and *photoionized* plasma. The first corresponds to a nonequilibrium two-temperature plasma where the Rydberg states are occupied due to the collisional transitions of free electrons with the bound states of discrete spectrum in the presence of inelastic interaction with the neutral components of medium [7]. In this case, the electron temperature can vary from 1000 to 3500 K [12], while the medium temperature of this layer can vary from 200 to 300 K, depending on its altitude. Note that this occupation mechanism prevails for the Rydberg states in the lower D layer. The electron thermalization is mostly due to the vibrational excitation of molecular nitrogen with the formation of an intermediate negative ion:

$$e^- + N_2(\mathrm{v} = 0) \rightarrow N_2^- \rightarrow e^- + N_2(\mathrm{v} \geq 1).$$

Rydberg states are occupied at the energies higher than certain energy E_* in a two-temperature quasistationary nonequilibrium plasma [7]. In the low ionosphere, it is determined by the action of electron flows precipitated from the ionosphere subjected to strong geomagnetic disturbances. Under these conditions, the distribution of occupancies over levels E_n near the ionization limit is characterized by the temperature close to temperature T_e of free electrons. At higher binding energies, $E_n \sim E_*$, the Rydberg states are almost unoccupied in the energy interval $\Delta\,E \;<< E_*$. This interval is called the narrow site of recombination flow or “neck of flow”.

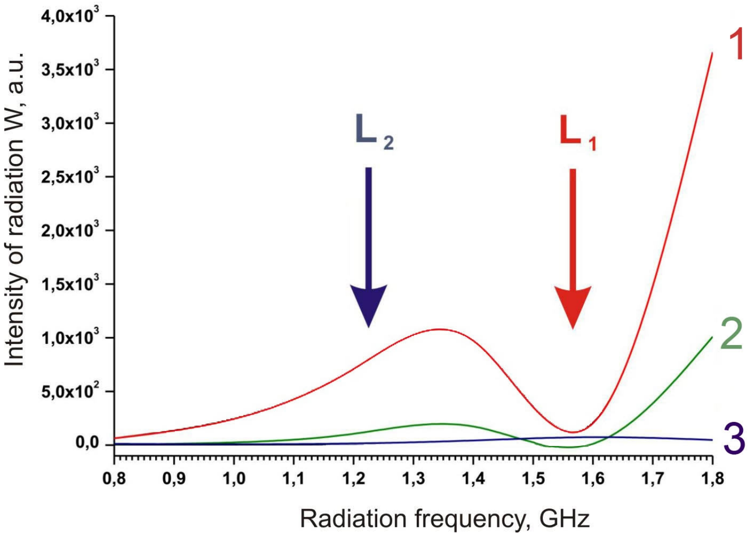

Fig. 3. The spectrum of UHF radiation for a quiet ionosphere (the electron density is $n_e = 10^3 \mathrm{cm}^{-3}$). Curve (1) corresponds to electron temperature T$_e$=1000 K and medium concentration $\rho_a = 10^{12} - 10^{13} \mathrm{cm}^{-3}$; (2) T$_e$= 1000 K, $\rho_a = 10^{14} \mathrm{cm}^{-3}$; (3) T$_e$= 2000 K, $\rho_a = 10^{12} - 10^{13} \mathrm{cm}^{-3}$

Above the neck, $E_n \geq E_*$, the collisional transitions between the binding states and continuum prevail. The radiative transitions resulting in the equilibrium occupation of the low-lying states with temperature T_a of medium molecules dominate below the neck.

The diagram of emission lines dependent on the principal quantum number $n$are shown in Fig. 2 for the $L \rightarrow n$ transitions between the split-out and degenerate Coulomb levels and the possible $L \rightarrow L'$ transitions between the split-out levels of quasimolecules $A**N_2$ and $A**O_2$, as calculated in [8]. Regard to the radiation intensity calculation we have taken into account dipole transitions only, i.e. with common selection rules ($\Delta l = \pm 1$), as it is usually done in the presence of superposition of states. For each quasimolecule, the distribution of n-dependent emission lines in the range 0.8-10 GHz contains four sets of lines corresponding to the $L \rightarrow L'$ transitions converging, with increasing L', to the $L \rightarrow n$ transition, where L =0, 1, 2, 3. These transition lines are symbolized as $N_{LL'}$, N_{Ln}, and $O_{LL'}$, O_{Ln} for the quasimolecules $A**N_2$ and $A**O_2$, respectively. One can see that the relative frequency shift for the limiting N_{Ln} and O_{Ln} occurs in three spectral ranges where the transitions are suppressed for small n values. The reason is that the characteristics of slow-electron scattering from the nitrogen and oxygen molecules are different.

The frequency dependence of the intensity of incoherent UHF radiation from an excited medium in the range 0.8-1.8 GHz is shown in Figs. 3 and 4 for a quiet and disturbed ionosphere. One can see that the UHF-radiation profile is a nonmonotonic function of frequency ω and rises steeply near the right boundary of the range. With a two-order increase in the electron concentration n_e the relative intensities W increase approximately by a four order of magnitude. This has a direct relationship to the observed effect of sequential decrease in the signal-to-noise ratio for the L_1 and L_2 GPS signals with increasing flare intensity [2], because the first frequency range 1.17-1.71 GHz of decrease virtually coincides with the "transparency window" for the propagation of the satellite signals.

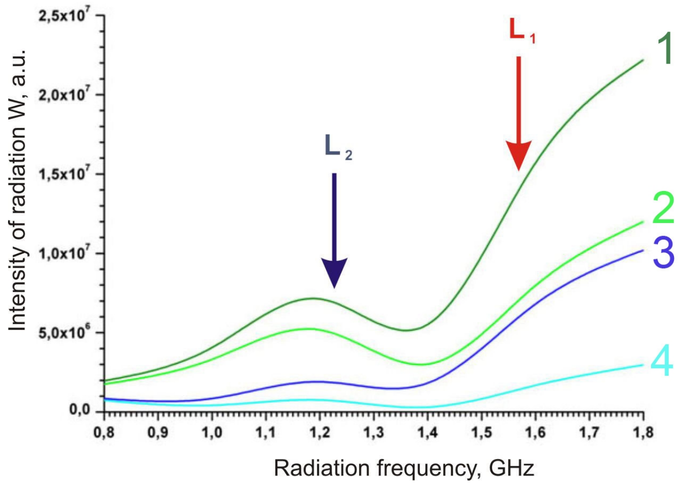

Fig. 4. The spectrum of UHF radiation for a disturbed ionosphere (the electron density is $n_e = 10^5 \text{cm}^{-3}$). Curve (1) corresponds to electron temperature T_e=2000 K and neutral medium concentration $\rho_a = 10^{12} - 10^{13} \text{cm}^{-3}$; (2) T_e= 2000 K, $\rho_a = 10^{14} \text{cm}^{-3}$; (3) T_e= 3000 K, $\rho_a = 10^{12} - 10^{13} \text{cm}^{-3}$; (4) T_e= 3000 K, $\rho_a = 10^{14} \text{cm}^{-3}$

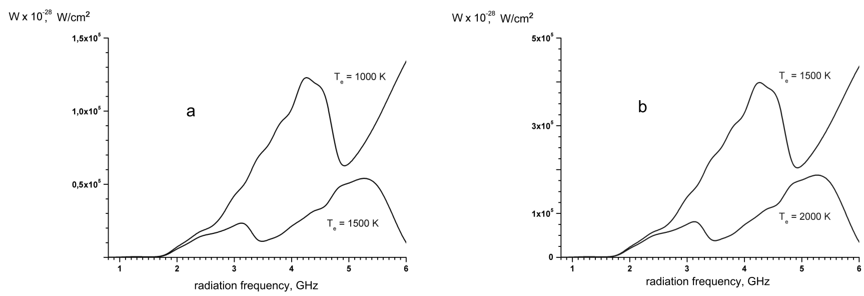

Fig. 5. The power flux W as a function on the frequency ν, density n_e, and temperature T_e: (a) $n_e = 5{\cdot}10^3$ cm^{-3}, T_e= 1000 K and T_e= 1500 K (the morning, calm conditions);(b) $n_e = 10^4$ cm^{-3}, T_e= 1500 K and T_e= 2000 K (daytime, calm conditions)

Additional background radiation in the range 4.0 – 6.0 GHz

As shown in Figures 5(a, b), the next minimum of power flux intensity is located near the frequency 5 GHz. In contrast, it is due first minimum radiative transitions is more stable when the plasma parameters. By increasing of temperature T_e the curve character is changed to inverse and becomes weakly dependent on a frequency. A behavior of the curves converging to a single point is called the “bottleneck”. This dependence of the power flux radiation under the small change in temperature provides signal delay at a given GPS frequency, not exceeding 10% of difference between the lower and the upper curve from the change of temperature on 500K, on the assumption that the delay signal proportional to the intensity of background radiation. This is illustrated clearly in the Table, where the ratio of the power radiation fluxes $\eta = W(T_e^<)/W(T_e^>)$ is shown for different values n_e and T_e at the frequency $\nu_f^{(2)} = 5$GHz. The value $\eta = 2$ for the electron density $n_e = 5 \cdot 10^4$ cm^{-3} is the boundary of transition to a strong increase of the delay. The calculations are performed in the framework of the ”Rydberg”program taking into account depending on the electron density distribution in height [13]. Thus, the emitting layer in decimeter range is located in the interval of 90-110 km.

Note that the ratio of the power radiation fluxes at the first $\nu_f^{(1)} = 1.57$ GHz frequency for the electron density $n_e = 10^4$ cm^{-3} and the range of T_e from 2000K to 3000K

Table 1. The dependence of ratio $\eta = W(\nu_f^{(2)},\ n_e,\ T_e^{<})/W(\nu_f^{(2)},\ n_e,\ T_e^{>})$ on the electron density n_e for a given frequency $\nu_f^{(2)}$

n_e, 10^3 cm^{-3}	5		10		20		50	
	$T_e^{<} =$ 1000K	$T_e^{>} =$ 1500K	$T_e^{<} =$ 1500K	$T_e^{>} =$ 2000K	$T_e^{<} =$ 2000K	$T_e^{>} =$ 2500K	$T_e^{<} =$ 2500K	$T_e^{>} =$ 3000K
η	1.09		1.18		1.03		2.0	

reaches the $\eta = 2$ value also. Under these conditions, the point $\nu_f^{(1)}$ is located on the steep slope of the curve $W(\nu_f)$ (see Fig. 4). The ratio of power radiation fluxes is 1.08 for the next $\nu_f^{(2)} \approx 5$ GHz frequency range corresponding to the minimum of the upper curve $W(\nu_f,\ T_e^{<})$ and the slanting behavior of the lower $W(\nu_f,\ T_e^{>})$ one at electron density $n_e = 2 \cdot 10^4$ cm^{-3} for the said temperature T_e range. The $\nu_f^{(2)} \approx 5$ GHz frequency is more preferable in relation to the first one by using in system GPS, because the difference module $\Delta W(\nu_f) = |W(\nu_f,\ T_e^{<}) - W(\nu_f,\ T_e^{>})|$ is important for the satellite signal stability only. No less important it is the fact that the frequency bandwidth around of the minimum value is much greater than the width of the first one and therefore should be more informative. Under conditions of strong geomagnetic disturbance (for $n_e \geq 10^5$ cm^{-3}) additional background UHF radiation at the $\nu_f^{(2)}$ frequency increases strongly and passes onto the inclined portion of the curve, which leads to the problem of identification of the signal.

Analysis of the data indicates that the delay signal at a frequency of 5 GHz may be recovered from the power spectrum of infrared radiation, which to be measured in a spectrometer mounted on a GPS-satellite constellation. At the same time, using of the all possible methods of filtering the signal at the 1.57 GHz frequency cannot eliminate the position errors since the delay is due to the resonance cascade of re-radiation of the GPS signal on the Rydberg states. Note that estimation of the signal delay by the additional background UHF radiation of lower ionosphere essentially impossible here, because in contrast to the IR radiation level of its power is significantly lower than the thermal noise floor. This can be done on the basis of infrared radiation, as his power is several orders higher than the power UHF radiation of Rydberg states [7]. Indeed, since the position of the "bottleneck" at $\nu_f^{(2)}$ frequency proportional to the electron density n_e, and does not depend on the temperature T_e (see Figure 5), the amount of signal delay can be estimated by recovering population of Rydberg states by IR spectrum.

Photoionized plasma

The photoionized plasma is produced under the action of a broadband radiation coming from the solar flare within 20-30 min. This process is caused by the multiquantum excitation of the electronic states of atoms and molecules where the spin forbidding is removed for the corresponding radiative transitions because of the interaction with medium molecules M. The distinction between the populations of high-lying Rydberg states (with high values of n) and the situation in the nonequilibrium recombining plasma is that the former are additionally depleted due to photoionization. At small n, the Rydberg and low-lying excited states are depleted due to the predissociation processes, including the nonadiabatic transitions via the intermediate valence configurations and the resonance (nonresonance) transfer of internal energy as a result of the collisional processes followed by the thermalization of medium. This is evident from the rise in its temperature with increasing altitude in the range 40-60 km. It is significant that the l - mixing process for these states is strongly suppressed, and the influence of medium is significantly reduced [11]. This is particularly important for the formation of frequency profile of the IR radiation [7], as measured in [4]. A direct indication of this fact is the presence of a characteristic decrease in intensity with increasing frequency radiation on the position of the first peak (with a wavelength of about 20 microns) to low (close to 15 microns), which is associated with the process l - mixing. It should be also pointed out that the IR radiation coming from the altitudes higher than 120 km cannot, basically, have such a relief structure.

The distinction between the actions of the photoionized and recombining plasma on the distortion of satellite GPS signals and the attendant errors in positioning is clearly seen from the observed time dependence of positioning error. In the first case, a sharp and short-lived (down to 20 min) peak appears with an positioning error of more than 50 m). The second case corresponds to the formation of a bell-shaped dependence with a characteristic width of several hours and positioning error of 15-20 m.

The propagation of the satellite GPS signal is accompanied by two physical processes. The first is associated with the resonance absorption followed by induced reemission of an electromagnetic wave from the Rydberg states of quasimolecules $A{*}{*}N_2$ and $A{*}{*}O_2$ with a time delay of $10^{-5} - 10^{-6}$s in one scattering event. The second one is caused by the incoherent plasma radiation. These processes superpose independently on one another. The most characteristic feature of the resonance absorption of electromagnetic wave followed by radiation is that the envelope of resonance intensity profile rises by a factor of 2-3 and the phase shift forms. It is precisely these two processes that are responsible for the increase in intensity and disappearance of the GPS signal, as observed in [3]. This indicates that the emitted and received signals differ from one another.

Conclusion

Thus, the physical cause of the time delays and phase shifts in the signals received from the global navigational satellite systems is associated with a cascade of resonance reemission from the Rydberg states of quasimolecules $A**N_2$ and $A**O_2$ in the atmospheric E and D layers; i.e., it is dictated by the quantum properties of medium in which the signal propagates. Note in conclusion that the systematic analysis of the long-wave portion of IR spectrum observed in [4] (for the $\Delta n = 1$ transitions) from the radiating D layer over a long period of time under conditions of strong magnetic storms should be an independent line of investigation. This spectral range falls on the interval $10 < n < 40$ of principal quantum numbers, where the l-mixing process is effective enough [14]. The above-listed features of frequency profile should appear in this case as well. As distinct from the radiation from the $A**N_2$ and $A**O_2$quasimolecules in the decimeter range ($\Delta n = 0$ transitions), the spectral pattern of the $n\,L \rightarrow (n-1)\,L'$ transitions should be more cumbersome. This fact can form a basis for the IR layerwise scanning of D layer and diagnostics of plasma parameters, including the determination of the Rydberg state populations. Simultaneous calculation in frame of the UHF radiation theory [8] and measurement in real-time data on the long-wave infrared radiation will solve this problem only. Positioning errors of the GPS may be used to determine key ionospheric parameters: temperature and electron density, concentration of neutral medium component, etc.

References

1. http://gps.ece.cornell.edu/realtime.php

2. *Cerruti A.P., Kintner Jr. P.M., Gary D.E., et al.* Effect of intense December 2006 solar radio bursts on GPS receivers. // Space Weather. – 2008. V. 6. - S10D07.

3. *Afraimovich E.L., Astafieva E.I., Berngardt O.I., et al.* Mid-latitude amplitude scintillation of GPS signals and GPS performance slips at the auroral oval boundary. // Radiophysics and Quantum Electronics. – 2004. - V. 47. - N 7. - P.453-468.

4. *Mlynczak M.G., D.G. Johnson D.G., Latvakovski H., et al.* First light from the far-infrared spectroscopy of the troposphere (FIRST) instrument. // Geophys. Res. Lett. – 2006. - V. 33. - L07704.

5. *Thessin R.N.* Atmospheric signal delay affecting GPS measurements made by space vehicles during launch, orbit and reentry. - California: Massachusetts Institute of Technology, 2005. 186 P. - dspace.mit.edu/handle/1721.1/33211

6. *Golubkov G.V., Manzhelii M. I., Karpov I.V.* Chemical Physics of the Upper Atmosphere. // Russian Journal of Physical Chemistry B. - 2011. - V. 5. N 3. - P. 406-411.

7. *Golubkov G.V.* Influence of the medium on the electromagnetic radiation spectrum of highly excited atoms and molecules. // Russian Journal of Physical Chemistry B. – 2011. - V. 5. - N 6. - P. 925-930.

8. *Golubkov G.V., Golubkov M.G., Manzhelii M.I.* Microwave radiation in the upper atmosphere of the earth during strong geomagnetic disturbances. // Russian Journal of Physical Chemistry B. – 2012. V. 6. - N 1. - P. 112-127.

9. *Golubkov G.V., Golubkov M.G., Manzhelii M.I.* Microwave and IR radiation of the upper atmosphere during periods of enhanced solar activity. // Doklady Phisics. - 2012. - V. 57 - No. 12. - P. 461-464.

10. *Avakyan S.V.* Physics of the solar-terrestrial coupling: Results, problems, and new approaches. // Geomagn. Aeronomy. – 2008. - V. 48. N 4. - P. 417-424 (2008)

11. *Golubkov G.V., Golubkov M.G., Ivanov G.K.* Rydberg States of Atoms and Molecules in a Field of Neutral Particles. In: The Atmosphere and Ionosphere: Dynamics, Processes and Monitoring. / Eds. V.L.Bychkov, G.V.Golubkov, A.I.Nikitin. New York: Springer, 2010. - P. 1-68.

12. *Oyama K.I., Abe T., Mori H. et al.* Electron temperature in nighttime sporadic E layer at mid-latitude. // Ann.Geophys. – 2008. - V. 26. - P.533-541.

13. *Barabash V., Osepian A., Dalin P. et al.* Electron density profiles in the quiet lower ionosphere based on the results of modeling and experimental data. // Ann. Geophys. – 2012. - V. 30. - N 9. - P. 1345-1360.

14. *Golubkov, G.V., Ivanov G.K., Balashov E.M., Golubkov M.G.* l-mixing and dissociation of Rydberg molecules accompanying slow collisions with inert-gas atoms. // JETP – 1998. - V. 87. - N 1. - P. 56-63.

Дециметровое и инфракрасное излучения нижней ионосферы в периоды повышения солнечной активности

Голубков Г.В., Манжелий М.И.

Институт химической физики им. Н.Н. Семенова РАН, Россия

Во время геомагнитных возмущений в E- и D-слоях ионосферы происходит значительный отрыв электронной температуры T_e от температуры среды T_s, т.е. $T_e << T_s$. В результате устанавливается двухтемпературная слабоионизованная рекомбинационная плазма, параметры которой достаточно надежно определяются на основании прямых ракетных измерений. Так как частота соударений электронов с нейтральными частицами среды порядка $10^{12} - 10^{14}$ с$^{-1}$, в плазме формируются два локальных распределения по энергиям дискретных состояний атомов и молекул. Первое (с температурой T_e) соответствует высоковозбужденным ридберговским состояниям, расположенным выше некоторой энергии E_* (горлышка стока). Она находится из условия минимума константы скорости тушения за счет переходов в нижележащие состояния. Второе (с температурой среды T_s) относится к низколежащим состояниям. Положение узкого места находится из условия минимума константы скорости тушения за счет переходов в нижележащие состояния.

В докладе обсуждаются основные механизмы процессов заселения и тушения ридберговских состояний в рекомбинационной двухтемпературной плазме. Важнейшим из них является процесс l-перемешивания, приводящий к образованию орбитально вырожденных квазимолекул $A^{**}N_2$ и $A^{**}O_2$. Заселенности ридберговских состояний квазимолекул зависят от концентрации среды, потока и температуры электронов. Рассмотрен спектр некогерентного излучения дециметрового диапазона для переходов между расщепленными уровнями этих квазимолекул. Показано, что он является неоднородным и содержит три диапазона частот, в которых происходит заметное уменьшение интенсивности излучения. Физическая причина формирования этих диапазонов обусловлена сдвигом спектров излучения квазимолекул, содержащих невозбужденные молекулы N_2 и O_2. Образование ридберговских квазимолекул сопровождается интенсивным сверхфоновым инфракрасным (ИК) излучением, по спектру которого можно восстанавливать послойные распределения заселенностей ридберговских частиц в D- и E-слоях атмосферы.